



Valerica Moșneguțu, Ligia Munteanu

Localized Modes at Defects in Sonic Composites

The paper discusses a sonic composite with a linear defect. Such structures allow localization of modes in the vicinity of the line defect with propagation along this line. The material in the vicinity of the line behaves like frequency-specific mirrors. The waves are trapped in a virtual set of mirrors parallel to the defect line, and the propagation bounce back and forth between these mirrors. The mirrors localize waves within a finite region of the line defect, and modes are quantized into discrete frequencies. If a mode has a frequency in the gaps, then it must exponentially decay inside the material. In a similar fashion, if the materials have point defects, the waves can be localized at the surface in which these point defects are located.

Keywords: *sonic composite, full band-gap, linear defects*

1. Introduction

A conventional sonic composite is a finite size periodic array composed of scatterers embedded in a homogeneous material. The existence of a large sound attenuation band is due to the superposition of multiple reflected waves within the array according to Bragg's theory, and consequently, it is connected to a large acoustic impedance ratio between the scatterer and the matrix materials, respectively.

Bragg reflections occurring at different frequencies inverse proportional to the central distance between two scatterers are the key of the band-gaps. If the band-gaps are not wide enough, their frequency ranges do not overlap. These band-gaps can overlap due to reflections on the surface of scatterers, as well as the wave propagation within the scatterers. Then, any wave is reflected completely from this periodic array in the frequency range where all of band-gaps for different periodical directions overlap. This is the fundamental mechanism for the formation of a full band-gap which is required for sonic composites. The complete reflection on the boundaries of scatterers is due to the full band-gap property itself, independent of the incident angle. This makes sharp bends of the wave-guide in

the sonic composite [1, 2]. The evanescent waves are distributed across the boundary of the waveguide into the surrounding composite [3-6].

The key of the band-gap generation in sonic composites is the lack of purely real wave vector for certain modes of waves at certain frequencies. The wave amplitude may decay exponentially sustaining an evanescent mode, or can increase exponentially and a defect can terminate this exponential growth to sustain also an evanescent mode [7].

The primary goal of this paper is to analyze a sonic composite periodic along axes with a linear defect, i.e. a plate consisting of 160 local spherical shells resonators made from auxetic material, of internal and external radii R_1 and R_2 . The length of the plate is L , its width is d , while the thickness of the plate is $2R_2 \leq e \leq 3R_2$. A linear defect of size $(5R_2/2, d/2, e/2)$ is located in the middle of the plate (Figure 1). Such structure allows localization of modes in the vicinity of the line defect with propagation along this line [8].

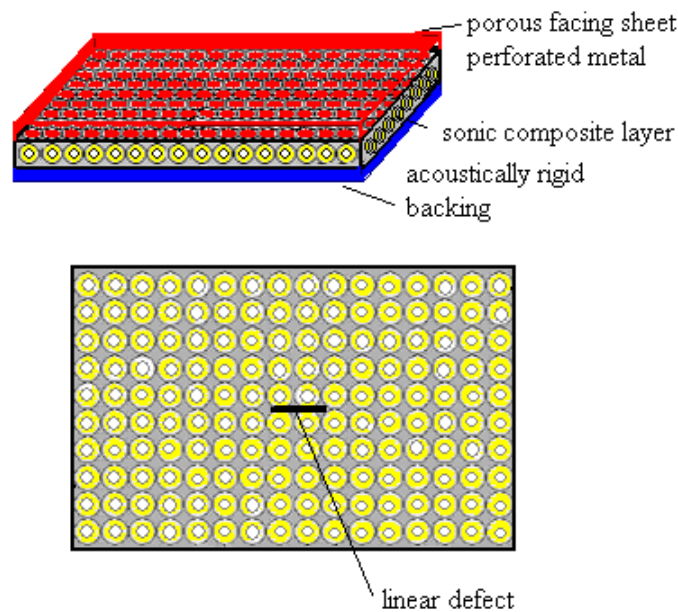


Figure 1. Sonic plate with spherical shells resonators made from auxetic material and a defect located in the middle of the plate

Materials with a negative Poisson ratio ν are auxetic materials. Auxetic behavior is found in materials from the molecular and microscopic levels, up to the macroscopic level. The term auxetic is coming from the Greek word "auxetos" meaning that "which may be increased". Instead of getting thinner like an elon-

gated elastic band, the auxetic material gains volume, expanding laterally when stretched. All the major classes of materials (polymers, composites, metals and ceramics) can exist in auxetic form. Typically mechanical properties (for example, the indentation resistance and shear modulus) are inversely proportional to $(1-v^2)$ or $(1+v)$. The negative limit of v for isotropic materials is -1, and $(1-v^2)$ or $(1+v)$ tends to zero, leading to enhancements in the material property for auxetic materials in comparison with the non-auxetic ones.

2. The theory

The auxetic material can be described by the Cosserat theory [9]. Classical mechanics fails in describing the mechanical behavior of auxetic materials under deformation. The Cosserat, micropolar and classical theories of elasticity are continuum theories, which make no reference to atoms or other structural features of the material. Elasticity theory represents more than an analytical description of the phenomenological behavior since it can be derived as a first approximation of the interaction between atoms in the solid [10].

Interatomic forces are of short range; but they exert more influence than one atomic space. The characteristic length l in this case should be on the order of the atomic spacing. Phenomena associated with micropolar elasticity are likely to be of larger magnitude, and therefore of greater interest in materials such as cellular solids with larger scale structural features. The equations of motion in the absence of body forces and body couples are

$$(1) \quad \sigma_{kl,k} - \rho \ddot{u}_l = 0, \quad m_{rk,r} + \varepsilon_{klr} \sigma_{lr} - \rho j \ddot{\varphi}_k = 0.$$

Here σ_{kl} is the stress tensor, m_{kl} is the couple stress tensor, u is the displacement vector, φ_k is the microrotation vector which in Cosserat elasticity is kinematically different from the macrorotation vector $r_k = 1/2 \varepsilon_{klm} u_{m,l}$, and ε_{klm} is the permutation symbol. We remember that φ_k refers to the rotation of points themselves, while r_k refers to the rotation associated with movement of nearby points.

In (1) ρ is the mass density and j the microinertia. The constitutive equations are given by

$$\sigma_{kl} = \lambda e_{rr} \delta_{kl} + (2\mu + \kappa) e_{kl} + \kappa \varepsilon_{klm} (r_m - \varphi_m) + C_1 \varphi_{r,r} \delta_{kl} + C_2 \varphi_{k,l} + C_3 \varphi_{l,k}, \quad (2)$$

$$m_{kl} = \alpha \varphi_{r,r} \delta_{kl} + \beta \varphi_{k,l} + \gamma \varphi_{l,k} + C_1 e_{rr} \delta_{kl} + (C_2 + C_3) e_{kl} + (C_3 - C_2) \varepsilon_{klm} (r_m - \varphi_m), \quad (3)$$

where $e_{kl} = 1/2(u_{k,l} + u_{l,k})$ is the macrostrain vector. λ and μ are Lamé elastic constants, κ is the Cosserat rotation modulus, α, β, γ , the Cosserat rotation gradient moduli, and $C_i, i=1,2,3$ are the chiral elastic constants associated

with noncentrosymmetry. For $C_i = 0$ the equations of isotropic micropolar elasticity are recovered. For $\alpha = \beta = \gamma = \kappa = 0$, eq. (1) reduces to the constitutive equations of classical isotropic linear elasticity theory. From the requirement that the internal energy must be nonnegative (the material is stable), we obtain restrictions on the micropolar elastic constants $0 \leq 3\lambda + 2\mu + \kappa$, $0 \leq 2\mu + \kappa$, $0 \leq \kappa$, $0 \leq 3\alpha + \beta + \gamma$, $-\gamma \leq \beta \leq \gamma$, $0 \leq \gamma$, and any positive or negative C_1, C_2, C_3 .

Consider the sonic plate with spherical shells resonators made from auxetic material and a defect located in the middle of the plate. For simplicity, without any loss of generality, the particular 2D case in which all quantities depend only on the propagation direction Ox of waves and the normal Oz on the plate.

The general solution of (1)-(3) can be written as

$$U = U_{\text{lin}} + U_{\text{nonlin}}, \quad (4)$$

where the linear and nonlinear terms express the linear and nonlinear superposition of cnoidal functions, respectively,

$$U_{\text{lin}} = 2 \sum_{k=0}^n \alpha_k \text{cn}^2(\xi_k; m_k), \quad U_{\text{nonlin}} = \frac{\sum_{k=0}^n \beta_k \text{cn}^2(\xi_k; m_k)}{1 + \sum_{k=0}^n \gamma_k \text{cn}^2(\xi_k; m_k)}, \quad (5)$$

with $0 \leq m_k \leq 1$, $\xi_k = k_{1k}x + k_{2k}y + k_{3k}z - \omega t$, and $\alpha_k, \beta_k, \gamma_k, \xi_k$, the unknown quantities. The state variables $U_j = (v_1, v_3, \phi_2, u_1, u_2)$, $j = 1, 2, \dots, 5$, of the problem are expressed under the form

$$U_j = 2 \sum_{k=0}^n \alpha_{kj} \text{cn}^2(\xi_{kj}; m_k) + \frac{\sum_{k=0}^n \beta_{kj} \text{cn}^2(\xi_{kj}; m_k)}{1 + \sum_{k=0}^n \gamma_{kj} \text{cn}^2(\xi_{kj}; m_k)}, \quad \xi_{kj} = k_{1kj}x + k_{2kj}y + k_{3kj}z - \omega t. \quad (6)$$

3. The band-gaps

The waves in periodic media can have propagation with no scattering and generation of the band-gaps. That means that in the band-gaps the waves (sound) are not allowed to propagate due to complete reflections. The band-gaps or the Bragg reflections occur at different frequencies inverse proportional to the central distance between two scatterers. If the band-gaps are not wide enough, their frequency ranges do not overlap. Consequently, any wave is reflected completely from this periodic structure in the frequency range where all the band-gaps for the different periodical directions overlap. This is the fundamental mechanism for the formation of a full band-gap.

The structure of the band-gap can be better understood via linear dispersion curve $\omega-k$, where ω is the angular frequency and k , the wave number. Note that no waves are allowed to propagate into the band-gap. The waves inside the band-gap are evanescent modes trapped in this region of frequencies.

The key observation is that the periodicity of the sonic material that induces a band-gap into its band structure. No waves are allowed into the band-gap. No real wave number exists for any mode at that frequency, i.e. the wave number is complex. In this case the modes are evanescent, decaying exponentially into the material.

We can use point-like defects to trap the waves. By using line defects, we can also guide the waves from one location to another. The basic idea is that the waves propagate in the waveguide with a frequency within the band-gap of the material are confined to, and can be directed along, the waveguide. This is the mechanism for the guiding of waves.

To illustrate these ideas, we turn to the sonic plate with spherical shells resonators and a defect located in the middle of the plate.

In Figure 2 we plot the first and the second band-gaps (blue regions) in the direction of propagation of the waves formed by the presence of the defect. The white regions correspond to waves that can propagate through the material. The reduced units for the frequency is $\omega R_2 / 2\pi c_0$, with c_0 the speed of sound in air.

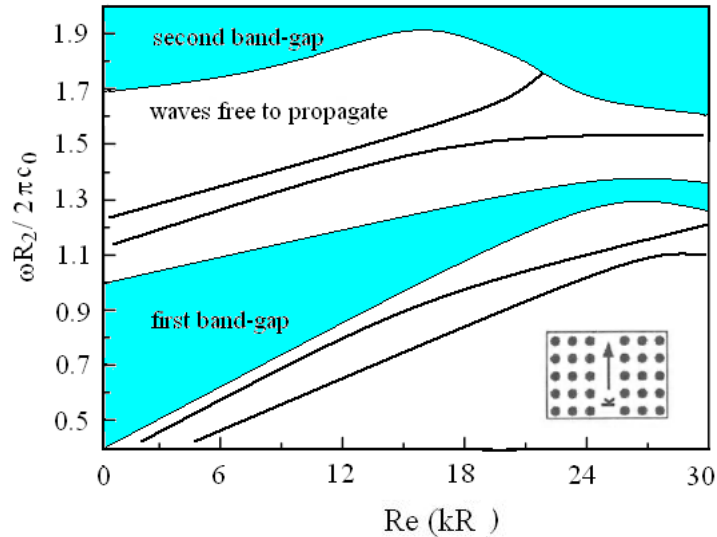


Figure 2. The band-gaps formed by the presence of the defect

The overlapping of all local band-gaps obtained from reflections on the scatterers as well as due to wave propagation in the scatterers, generates the full

band-gap. Any wave is reflected completely in the frequency range where all the local band-gaps for the different directions overlap. The rationale for of the band-gaps is the evanescent modes with purely imaginary wave vectors. The guided waves are accompanied by these evanescent waves which extend to the periodic array of scatterers surrounding the wave-guide. This is the fundamental mechanism for the formation of full band-gaps.

To understand the contribution of the first and second band-gaps to the final full band-gap obtained by overlapping of 100 band-gaps, we tried to see step by step, the generation of full band-gap in the range of frequencies $\omega R_2 / 2\pi c_0 \in [0.5, 1.9]$. Figure 3 shows the full band-gap (blue zone) generated by the overlap of 100 local band-gaps. The red zone corresponds to the first band-gap, and the green zone to the second band-gap. The red (green) lines inside the full band-gap define the borders of the corresponding local band-gaps.

We see that the contribution of the first band-gap to the formation of the full band-gap is quite important. The second gap makes a contribution only to the small values of $\text{Re}(kR_2)$. Inside the full band-gap the waves cannot escape. The line defect sustains the evanescent nodes and for a frequency inside the full band-gap, no real wave number exists for any mode at that frequency.

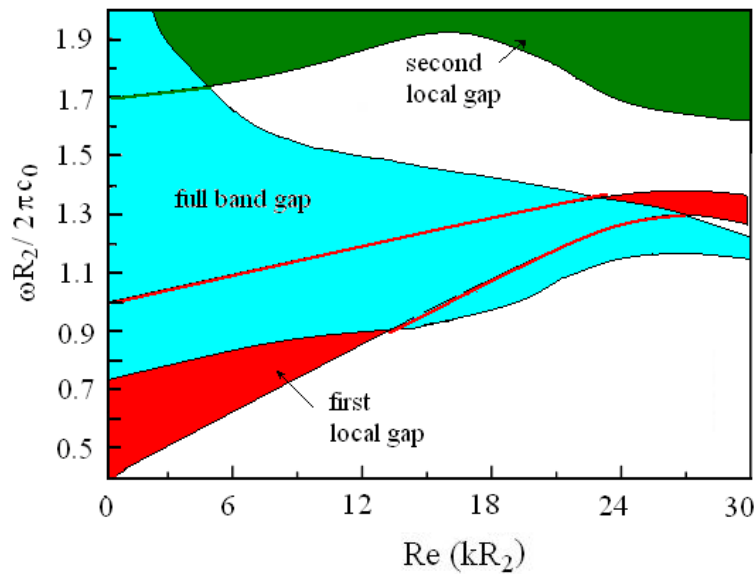


Figure 3. Full-band gap structure

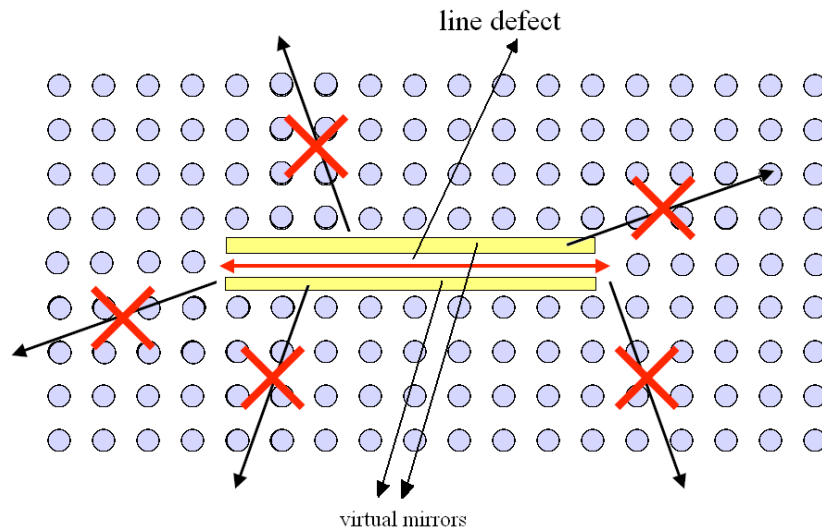


Figure 4. Waves are trapped in a virtual set of mirrors parallel to the defect line

Using a speech figure such as a metaphor, we can say that the waves are trapped in a virtual set of mirrors parallel to the defect line, and the propagation bounce back and forth between these mirrors. The mirrors localize waves within a finite region of the line defect, and modes are quantized into discrete frequencies.

Figure 4 schematically shows this idea. If a mode has a frequency in the gaps, then it must exponentially decay inside the material. In a similar fashion, the defects can terminate the evanescent modes with exponential growth, to sustain also an evanescent mode [11].

4. Conclusion

The paper discusses the role of a line defect to localization of modes in its vicinity. The waves are trapped in the region rounding the defect, and the modes are quantized into discrete frequencies. If a mode has a frequency in the gap, then it must exponentially decay inside the material. In a similar fashion, if the materials have point defects, the waves can be localized at the surface in which these point defects are located. If point defects are located near the external boundary of the material, the band-gap is only on one side of the surface because the exterior medium (air) does not have a band-gap.

Acknowledgement

The authors gratefully acknowledge the financial support of the National Authority for Scientific Research ANCS/UEFISCDI through the through the project PN-II-ID-PCE-2012-4-0023, Contract nr.3/2013.

References

- [1] Munteanu L., Chiroiu V., Donescu St., Brişan C., *A new class of sonic composites*, Journal of Applied Physics, 115, 104904, 2014.
- [2] Munteanu L., Chiroiu V., Serban V., *From geometric transformations to auxetic materials*, CMC: Computers, Materials & Continua, 42(3), 175-203, 2014.
- [3] Chiroiu V., Brişan C., Popescu M.A., Girip I., Munteanu L., *On the sonic composites without/with defects*, Journal of Applied Physics, vol. 114 (16), pp. 164909-1-10, 2013.
- [4] Hirsekorn M., Delsanto P.P., Batr, N.K., Matic P., *Modelling and simulation of acoustic wave propagation in locally resonant sonic materials*, Ultrasonics, 42, 231–235, 2004.
- [5] Munteanu L., Chiroiu V., *On the dynamics of locally resonant sonic composites*, European Journal of Mechanics-A/Solids, 29(5), 871–878, 2010.
- [6] Romero-García V., Sánchez-Pérez J.V., Garcia-Raffi L.M., *Evanescent modes in sonic crystals: Complex relation dispersion and supercell approximation*, Journal of Applied Physics, 108(4), 108-113, 2010.
- [7] Joannopoulos, J.D., Johnson, S.G., Winn, J.N., Meade, R.D., *Photonic Crystals*, Princeton University Press, second edition, 2008.
- [8] Munteanu L., Popescu M., *Effects of defects to the band-gaps generation*, PAMM- Proceedings in Applied Mathematics and Mechanics, 693-694, December 2014, work presented to 85th Annual Meeting of the International Association of Applied Mathematics and Mechanics (GAMM2014), March 10-14, 2014 Friedrich-Alexander Universität Erlangen-Nürnberg.
- [9] Donescu St., Chiroiu V., Munteanu L., *On the Young's modulus of a auxetic composite structure*, Mechanics Research Communications, 36, 294-301, 2009.
- [10] Cosserat E. and F., *Theorie des Corps Deformables*, Hermann et Fils, Paris, 1909.
- [11] Munteanu L., Chiroiu V., Sireteanu T., Ioan R., *Sonic multilayer composite films*, chapter 2 in Inverse Problems and Computational Mechanics, vol.2, Editura Academiei, 2015.

Addresses:

- Dr. Valerica Moşneguţu, Institute of Solid Mechanics, Romanian Academy, Ctin Mille 15, Bucharest 010141, valeriam732000@yahoo.com
- Dr. Hab. Ligia Munteanu, Institute of Solid Mechanics, Romanian Academy, Ctin Mille 15, Bucharest 010141, ligia_munteanu@hotmail.com